Current Research in Physiology 6 (2023) 100101

Contents lists available at ScienceDirect

Current Research in Physiology

journal homepage: www.sciencedirect.com/journal/current-research-in-physiology

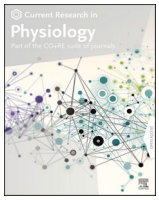

Precise CRISPR-Cas9-mediated mutation of a membrane trafficking domain in the *Drosophila* vesicular monoamine transporter gene

James D. Asuncion [a,b,c], Aditya Eamani [b], Ethan W. Rohrbach [b,c], Elizabeth M. Knapp [b], Sonali A. Deshpande [b], Shivan L. Bonanno [b], Jeremy E. Murphy [d], Hakeem O. Lawal [d], David E. Krantz [b,*]

[a] *Medical Scientist Training Program, David Geffen School of Medicine, University of California, Los Angeles, CA, 90095, USA*
[b] *Department of Psychiatry and Biobehavioral Sciences, David Geffen School of Medicine, University of California, Los Angeles, CA, 90095, USA*
[c] *UCLA Neuroscience Interdepartmental Program, University of California, Los Angeles, CA, 90095, USA*
[d] *Department of Biological Sciences, Delaware State University, Dover, DE, USA, 19901, USA*

A B S T R A C T

Monoamine neurotransmitters such as noradrenalin are released from both synaptic vesicles (SVs) and large dense-core vesicles (LDCVs), the latter mediating extrasynaptic signaling. The contribution of synaptic versus extrasynaptic signaling to circuit function and behavior remains poorly understood. To address this question, we have previously used transgenes encoding a mutation in the *Drosophila* Vesicular Monoamine Transporter (*dVMAT*) that shifts amine release from SVs to LDCVs. To circumvent the use of transgenes with non-endogenous patterns of expression, we have now used CRISPR-Cas9 to generate a trafficking mutant in the endogenous *dVMAT* gene. To minimize disruption of the *dVMAT* coding sequence and a nearby RNA splice site, we precisely introduced a point mutation using single-stranded oligonucleotide repair. A predicted decrease in fertility was used as a phenotypic screen to identify founders in lieu of a visible marker. Phenotypic analysis revealed a defect in the ovulation of mature follicles and egg retention in the ovaries. We did not detect defects in the contraction of lateral oviducts following optogenetic stimulation of octopaminergic neurons. Our findings suggest that release of mature eggs from the ovary is disrupted by changing the balance of VMAT trafficking between SVs and LDCVs. Further experiments using this model will help determine the mechanisms that sensitize specific circuits to changes in synaptic versus extrasynaptic signaling.

1. Introduction

Biogenic amines such as serotonin and dopamine regulate circuit function and behavior in both mammals and model invertebrates such as *Drosophila melanogaster*. While some amine receptors localize to classical synapses, many others localize to extrasynaptic sites (Fuxe et al., 2010). Amine release within classical synaptic structures is mediated by synaptic vesicles (SVs) which cluster at defined presynaptic release sites (Dittman and Ryan, 2019). Extrasynaptic release is thought to be mediated in part by large dense-core vesicles (LDCVs) which, unlike SVs, do not cluster at presynaptic active zones (Trueta et al., 2012). The requirement for each type of vesicle release for most aminergic circuits is not known.

Vesicular monoamine transporters (VMATs) are required for the storage of amines in both SVs and LDCVs (Blakely and Edwards, 2012). Rodents and humans contain two VMAT genes while *C. elegans* and *Drosophila melanogaster* contain only one (Liu and Edwards, 1997; Greer et al., 2005; Duerr et al., 1999). The *Drosophila* VMAT gene (*dVMAT*) encodes two RNA splice variants, dVMAT-A and dVMAT-B, which are expressed in neurons and a subset of glia, respectively (Greer et al., 2005; Chang et al., 2006; Romero-Calderón et al., 2008). We have used dVMAT-A as a model for VMAT trafficking since its C-terminal, trafficking domain appears similar to mammalian VMATs (Greer et al., 2005). Mutation of a tyrosine-based endocytosis motif or deletion of the distal C-terminus blocks rapid internalization of dVMAT-A from the cell surface in cultured cells and nerve terminals in vivo (Grygoruk et al., 2010, 2014). Mutation of the tyrosine motif or deletion of the distal C-terminus (the "Δ3" truncation mutant) also reduces the localization of dVMAT-A to SVs in vivo (Grygoruk et al., 2010, 2014). Both mutations also lead to a corresponding increase in the localization of dVMAT-A to LDCVs, although the trafficking events that cause the shift to LDCVs remains unclear (Grygoruk et al., 2010, 2014).

To study the behavioral effects of dVMAT-A trafficking in vivo, we have previously used mutant *dVMAT* transgenes encoding the tyrosine mutant or the C-terminal deletion to "rescue" the phenotype of a *dVMAT* null mutant (Grygoruk et al., 2014). Interestingly, some behaviors

* Corresponding author.
E-mail address: dkrantz@ucla.edu (D.E. Krantz).

https://doi.org/10.1016/j.crphys.2023.100101
Received 29 January 2023; Received in revised form 16 May 2023; Accepted 19 June 2023
Available online 20 June 2023

appeared to be severely compromised by shifting the relative amounts of dVMAT-A that localize SVs versus LDCVs, while others appeared to be minimally affected (Grygoruk et al., 2014; Wasserman et al., 2015). These data suggest that for some circuits, a precise balance of SV and LDCV release is essential, while for others, it is dispensable. However, we were concerned that by using transgenic expression constructs, some aspects of the mutant phenotype might be caused by non-physiological patterns of expression, or a mismatch with the endogenous developmental profile of *dVMAT*. The introduction of mutations into the endogenous *dVMAT* gene using CRISPR-Cas9 has the potential to circumvent these problems. In addition, avoiding the use of transgenes for dVMAT expression facilitates the introduction of other transgenic probes for optogenetics or live imaging, both of which will be useful for analyzing circuit activities potentially disrupted by changes in dVMAT trafficking.

Most *Drosophila* mutations generated via CRISPR-Cas9 have used double stranded (ds) homologous repair and vectors that include a screening marker, such as dsRED (Gratz et al., 2013; Sebo et al., 2013; Yu et al., 2013). Although the subsequent removal of dsRED or other markers can leave a small DNA scar, this is irrelevant for large deletions and "knock outs". By contrast, even a small scar can be disruptive if introduced within a coding sequence. The splice acceptor site for the last coding exon of dVMAT-A is adjacent to the trafficking domain, further increasing the risk for disrupting trafficking via mutations in this region. "Scarless"/"seamless" dsDNA repair represents one method to precisely introduce point mutants without introducing any other changes in the genomic DNA sequence (Xie et al., 2014; Ye et al., 2014; Gotze et al., 2022; Paquet et al., 2016). Single stranded (ss) DNA homologous repair represents an alternative approach and does not require the specific recognition sequence used for some ds scarless methods (Xie et al., 2014; Ye et al., 2014; Soldner et al., 2011; Yang et al., 2013). In addition, ss repair has been suggested to be less prone to random integration events and may be more efficient than ds methods (Boel et al., 2018).

Most ssDNA repair methods employ a relatively short (~100 bp) oligonucleotide, prohibiting inclusion of a cDNA encoding a visible marker to assist in screening transformants. Co-conversion techniques in which a second marker gene is mutagenized may be used to circumvent this problem (Levi et al., 2020), but necessitate the use of multiple

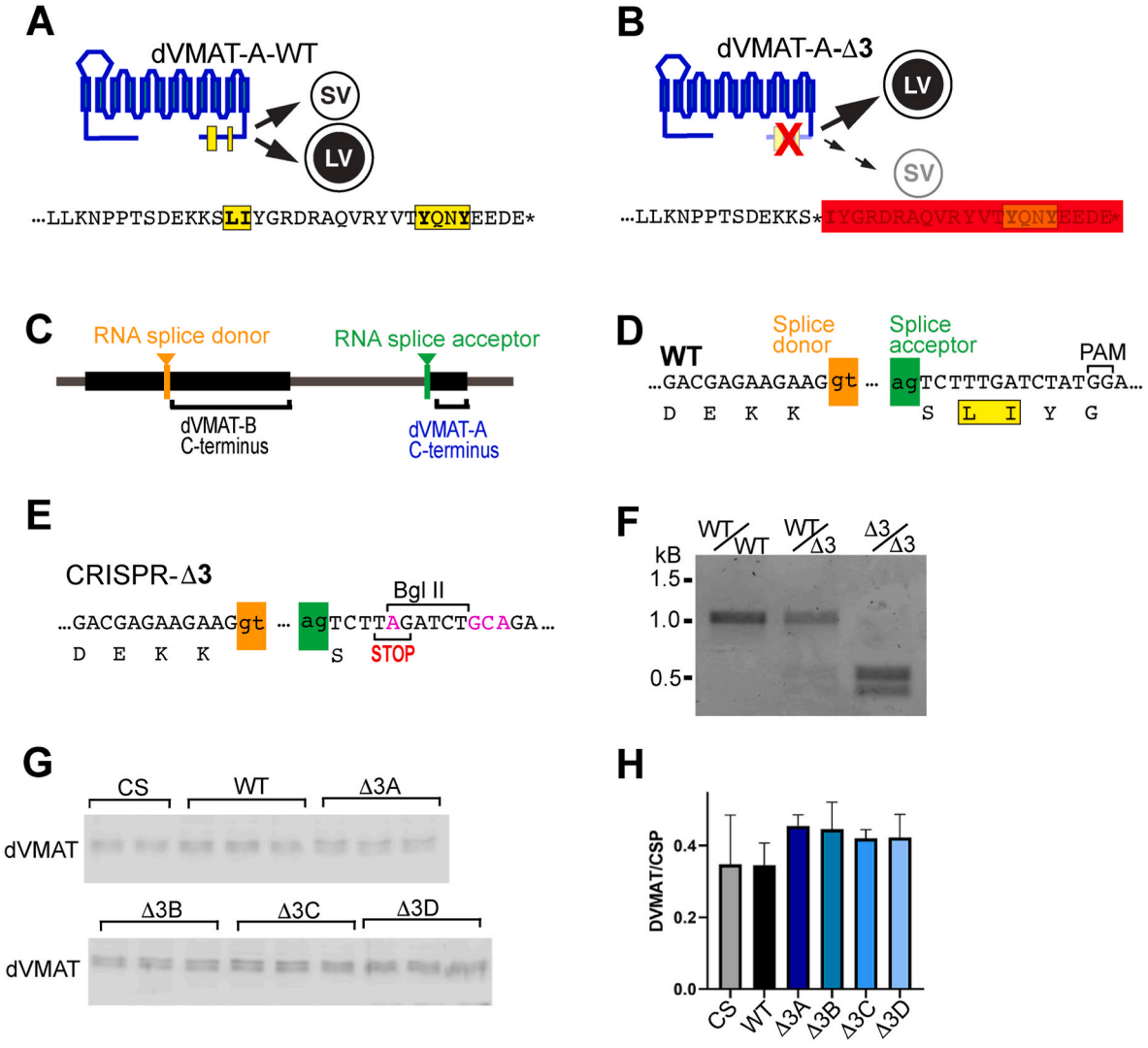

Fig. 1. CRISPR-Cas9 based mutagenesis and phenotypic screen for mutants.
A. The neuronal isoform of dVMAT (dVMAT-A) contains at least two trafficking motifs (yellow rectangles) within the C-terminal cytoplastic domain, which allow sorting to both synaptic vesicles (SVs) and large dense-core vesicles (LDCVs). B. Ablation of this domain disrupts dVMAT-A trafficking to SVs and increases trafficking to LDCVs. C. *dVMAT* gene expresses two splice variants. D. The splice acceptor site for dVMAT-A is proximal to a dileucine motif. E. The ssDNA repair construct mutated four base pairs (magenta). F. The BglII site allows cleavage of a PCR product in $dVMAT^{\Delta 3}$ that is uncut in WT.G. A western probed for DVMAT. H. Quantitation of the DVMAT bands normalized to a CSP loading control. (For interpretation of the references to colour in this figure legend, the reader is referred to the Web version of this article.)

sgRNAs and increase the possibility of off-target effects. Molecular screening techniques for point mutants also have been proposed (Touroutine and Tanis, 2020) and include the relatively simple addition of novel restriction sites into the repair vector (Cong et al., 2013).

We have taken an alternative strategy to precisely modify the *dVMAT* gene without a visible marker to identify founders, and used a primary phenotypic screen based on our prior experiments using *dVMAT* transgenes (Grygoruk et al., 2014). Since *dVMAT* transgenes that disrupt trafficking to SVs show reduced female fertility (Grygoruk et al., 2014), we reasoned that fertility could be used to screen for generation of the same mutation in the endogenous gene via CRISPR-Cas9. We report here the generation of the new allele $dVMAT^{\Delta 3}$. We have used the $dVMAT^{\Delta 3}$ mutation to analyze which sites within the oviposition circuit may be disrupted by changes in dVMAT trafficking.

2. Results

2.1. Generation of a dVMAT allele and phenotypic screening

dVMAT-A, the neuronal splice variant of dVMAT, contains dileucine and tyrosine-based trafficking motifs within the C-terminus (Fig. 1A) (Greer et al., 2005; Grygoruk et al., 2010, 2014). A *dVMAT-A* transgene lacking this region ("Δ3") showed reduced trafficking to SVs and increased trafficking to LDCVs (Fig. 1B) (Grygoruk et al., 2014). The splice acceptor site for the last coding exon of dVMAT-A is adjacent to a dileucine motif and the site used to introduce a stop codon in the Δ3 mutant (Fig. 1C and D) (Greer et al., 2005; Grygoruk et al., 2010, 2014). To introduce a stop codon at the same site within the endogenous *dVMAT* gene without disrupting the nearby DNA sequence, we designed a single stranded (ss) DNA repair construct. Four bases in total were changed (Fig. 1E, magenta) to introduce the stop codon, mutate the guide PAM, and introduce a silent BglII site to facilitate genotyping. Note that the premature stop codon is contained within the BglII site.

Our initial attempt using oligos with a total length of 200 bp failed (not shown), and others have suggested that, counterintuitively, shorter ssDNA oligos may be more effective (Yang et al., 2013). We therefore repeated the same procedure using an oligo with a total length of 90 bp (for sequence see Methods). One hundred embryos were injected with the guide RNA and ssDNA repair template to produce germline mosaics. Five progeny from each germline mosaic were mated to a balancer and backcrossed to generate 500 lines of which 450 survived. Homozygous females from each line were selected by the absence of the *Cy* marker and crossed to wild type males to assay for potential defects in female fertility. Of the 450 lines tested, 57 lines from 17 different germline mosaics exhibited a decrease in the number of eggs per vial by visual inspection.

As a secondary screen, we used PCR to amplify a 1-kb region bracketing the site of the mutation and the new BglII site. The presence of two bands at 460 and 580-bp rather than an uncleaved 1-kb PCR product indicated the presence of the BglII site and the premature stop codon (Fig. 1F). To confirm the presence of the mutated stop codon, genomic DNA was extracted from 57 candidates of the original 450 lines. Of the first 16 that were analyzed by PCR, seven were confirmed to contain the BglII site. The PCR products were then sequenced to determine whether the PAM site was also mutated and to rule out additional spurious mutations. The PCR products of the remaining 41 fly lines were subjected to Sanger sequencing to simultaneously interrogate all of the mutated sites. Of the 57 lines we sequenced, 23 contained the intended four base pair mutations without any additional changes. An additional 30 of the 57 lines (30/450 of total fly lines from 12 germline mosaics) contained missense mutations, insertions or deletions other than the intended changes. Four lines were false positives and later determined to be both genotypically and phenotypically wild type. We selected five of the sequenced lines for further analysis: four that contained the intended mutations without any additional spurious changes (Δ3A, Δ3B, Δ3C, Δ3D) and one that was genotypically and phenotypically wild type (WT). The WT control line was used as a genetically-matched control for later molecular and behavioral assays.

We probed the selected lines for dVMAT protein expression using a previously described antibody to the N-terminus of dVMAT-A (1G, H) (Romero-Calderón et al., 2008) and an anti-CSP loading control (1H). We did not detect a significant difference between the four $dVMAT^{\Delta 3}$ mutant lines, the WT control and an additional wild type (Canton S) control (Fig. 1G and H). These data are consistent with our previous observations using transgenic *dVMAT* mutants which indicate that disruption of fertility in response to altered trafficking can occur independent of any changes in expression levels (Grygoruk et al., 2014).

2.2. Phenotypic analysis

To more precisely quantitate the apparent defect in oviposition used for screening, we performed fertility (Fig. 2A) and fecundity (Fig. 2B) assays as previously described (Simon et al., 2008). Both fertility and fecundity were markedly reduced in lines containing the $dVMAT^{\Delta 3}$ mutant compared to control, but slightly higher than the null *dVMAT* mutant, which we have previously shown to lay few if any eggs (Simon et al., 2009) (Fig. 2A and B). By contrast, larval locomotion of the $dVMAT^{\Delta 3}$ mutant lines did not significantly differ from the genetically matched WT control or CS larvae (Fig. 2C).

Since the four $dVMAT^{\Delta 3}$ mutant lines behave similarly and showed similar levels of protein expression, we chose one (Δ3A) for further analysis. The survival of the Δ3A mutant line was reduced compared to the WT control (Fig. 2D) and showed a slight increase in feeding (Fig. 2E). These data are consistent with the results obtained using *UAS-DVMAT−Δ3* transgene to genetically rescue the *dVMAT* null and validate our previous observation that *dVMAT* trafficking mutants disrupt a subset of amine-dependent circuits, but have less severe effects on others (Grygoruk et al., 2014). Our current results also demonstrate the use of ssDNA repair and a phenotypic screen to introduce point mutations into a gene with a previously identified phenotype.

2.3. Site of the fertility defect

Some mutations that disrupt octopaminergic signaling cause defects in ovulation with retention of eggs within the ovary (Simon et al., 2009; Deady and Sun, 2015); by contrast, other mutants have been reported to primarily manifest defects downstream of ovulation and retain eggs within the calyx and oviducts (Cole et al., 2005). To specifically determine if $dVMAT^{\Delta 3}$ would show a defect in ovulation, we quantified the number of mature follicles and the distribution of eggs within the reproductive tract. We find that the ovaries in $dVMAT^{\Delta 3}$ mutant contain an elevated number of mature follicles relative to controls (Fig. 3A). In addition, most eggs were found in the ovaries in the mutant (Fig. 3B), in contrast to the controls and WT flies in general, in which eggs rapidly pass through the reproductive tract (Sun and Spradling, 2013). These data suggest that $dVMAT^{\Delta 3}$ causes a defect in ovulation (Deady and Sun, 2015).

The entire female reproductive tract in *Drosophila* is innervated by octopaminergic neurons from the ventral nerve cord, and multiple events in the reproductive tract in addition to follicle cell rupture are thought to be regulated by octopamine (White et al., 2021; Rezaval et al., 2014; Rodriguez-Valentin et al., 2006; Yoshinari et al., 2020; Pauls et al., 2018; Hana and Lange, 2017; Avila et al., 2012; Lee et al., 2003, 2009; Lim et al., 2014; Middleton et al., 2006). We have shown that octopamine regulates contraction of the lateral oviducts in *Drosophila* (Deshpande et al., 2022), raising the possibility that $dVMAT^{\Delta 3}$ might disrupt oviduct contractility. To test this, we introduced a transgenic probe for optogenetic stimulation into the $dVMAT^{\Delta 3}$ background. We used *Tdc2-LexA* to express the channelrhodopsin variant ChR2-XXL in octopaminergic neurons and optogenetically stimulated Tdc2+ neurons for 30 s. To help quantify contractions, we expressed the calcium reporter, RCaMP1b, in the oviduct muscles using

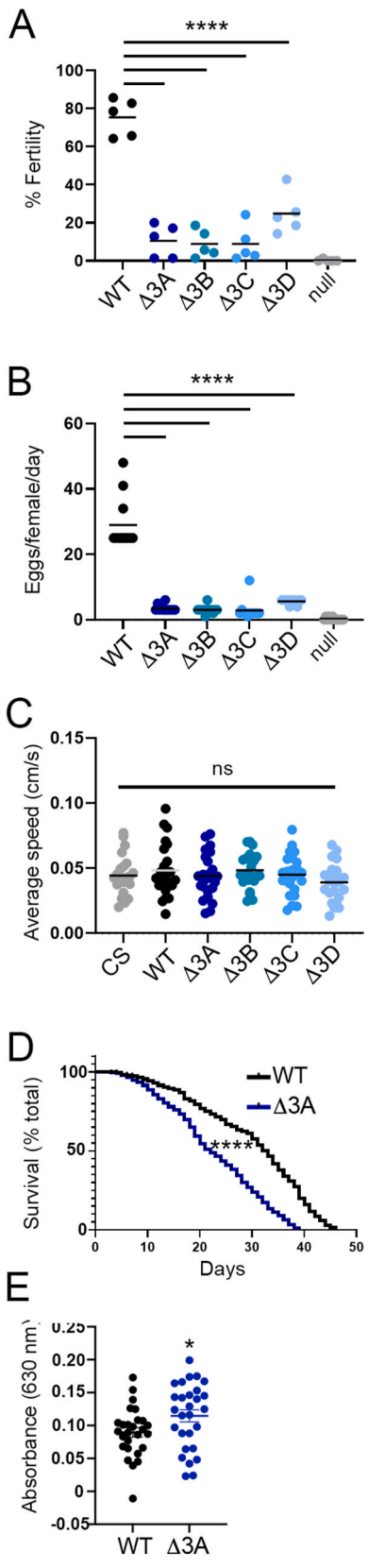

(caption on next column)

Fig. 2. Phenotypic analysis. Fertility (A), fecundity (B) and larval locomotion (C) were assayed for four genotypically verified *dVMAT*$^{\Delta 3}$ mutants, a WT control line genotypically wild type at the *dVMAT* locus and wild type Canton S flies (CS). One-way ANOVA with Bonferroni's multiple comparisons test, $p \leq 0.0001$****, mean indicated as horizontal lines. No significant differences in locomotion (C) were detected between mutant and wildtype larva (One way ANOVA). D. Adult survival on standard food was quantified for one of *dVMAT*$^{\Delta 3}$ alleles (Δ3A) and a WT control with Kaplan Meier analysis by Mantel-Cox Test, $p \leq 0.0001$****, N = 200 per group, median survival WT = 32.5 days, Δ3A = 22.0 days. E) Quantification via spectrophotometry of ingested blue dye (n = 27–28 groups of 10 flies), two-tailed unpaired *t*-test ($p \leq 0.0332$*). (For interpretation of the references to colour in this figure legend, the reader is referred to the Web version of this article.)

the muscle-specific driver *24B-GAL4*. To determine if the response would be depleted by multiple periods of stimulation, the stimulus was repeated a second time after a 30 s rest period. We did not detect a difference in the number of contractions between mutant and control during either of the stimulation periods (Fig. 3C).

3. Discussion

In vitro studies have revealed fundamental information about the molecular machinery responsible for transporter trafficking (Li et al., 2022; Wu et al., 2015; Moron et al., 2003; Xu et al., 2022; Ragu Varman et al., 2021; Sun et al., 2020). Additional in vivo models are required to determine the effects of transport on behavior and the contribution of the endogenous milieu to transport activity (Ingram et al., 2021; Bu et al., 2021; Fagan et al., 2020; Gowrishankar et al., 2018; Bowton et al., 2014; Meinke et al., 2022; Fischer et al., 2022; Kasture et al., 2019; Haase et al., 2021; Janickova et al., 2017). The expression of mutations as exogenous transgenes represents a powerful approach to determine how alterations in trafficking may disrupt behavior; however, transgenic expression systems may not fully capture the regulatory patterns of the endogenous gene. The use of transgenes for gene expression can also complicate the use of additional transgenic probes for neuronal stimulation and imaging. Here we report the use of CRISPR-Cas9 to disrupt trafficking signals in the C-terminus of the endogenous *dVMAT* locus, and initial phenotypic analysis of the new allele.

We screened a relatively large number of lines (450 total from 100 injected founders) to ensure that we would obtain a candidate. Although it is difficult to predict the efficiency of a given homologous repair construct, the number of candidates we obtained suggest that smaller phenotypic screens for other mutations may be sufficient, assuming that the oligo repair construct is optimized to ≤90 bp (Yang et al., 2013). We suggest that a phenotypic screen may be used to identify CRISPR-Cas9 mutants in other genes in cases in which standard marker-based screens using a dsDNA construct are not convenient, e.g., because a site for a scarless insertion is not apparent. In addition, the presence of DNA repeats can complicate the generation of the relatively large homology arms used for some ds repair constructs. Indeed, parallel attempts to generate a dsDNA construct for introduction of a premature stop codon in *dVMAT* were hampered by repeats in the 3' UTR (data not shown).

Consistent with our previous findings using a *dVMAT-Δ3* transgene, we find that the endogenous CRISPR-Cas9 mediated *dVMAT*$^{\Delta 3}$ mutation impairs female fertility and fecundity, but has no detectable effect on baseline, larval locomotion (Grygoruk et al., 2014). We also show retention of mature follicles in the ovaries, suggesting that loss of synaptic signaling or an increase in extrasynaptic signaling may disrupt follicle rupture. Follicle rupture is mediated by OAMB (Deady and Sun, 2015) and future experiments will more specifically explore the relationship between octopamine release by *dVMAT*$^{\Delta 3}$ and the response of OAMB receptors in follicle cells.

It is possible that *dVMAT*$^{\Delta 3}$ directly disrupts follicle cell rupture by changing octopamine release within the ovaries. Alternatively, it is

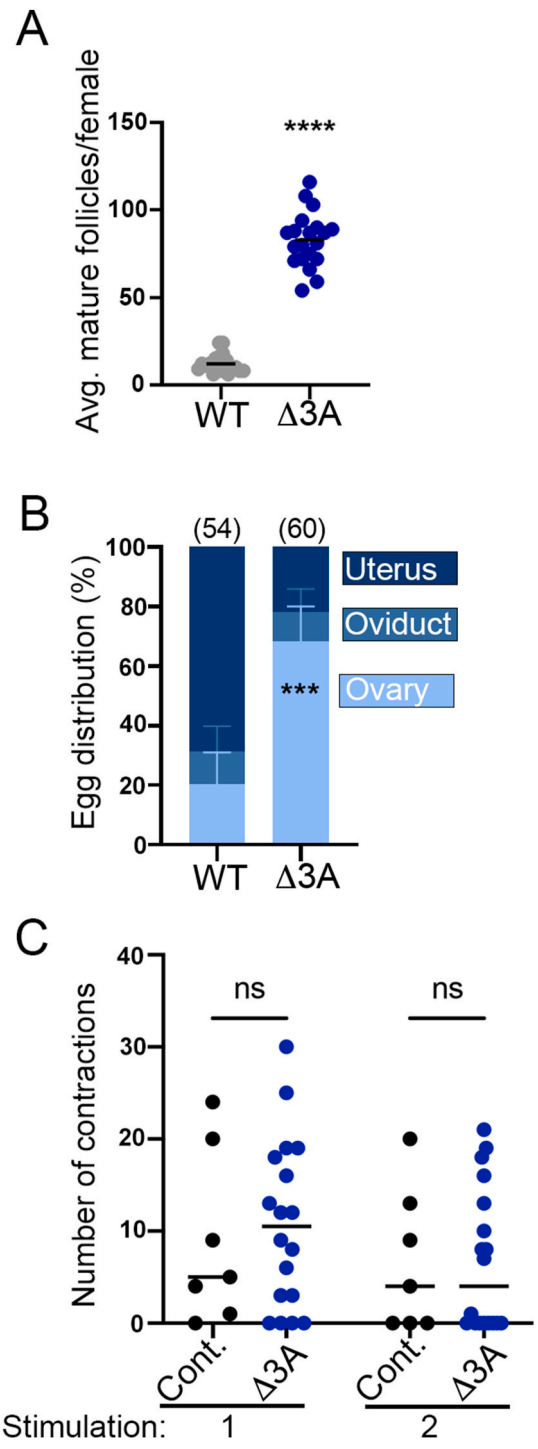

Fig. 3. *dVMAT*$^{\Delta 3}$ mutants retain mature eggs in their ovaries.
A. Quantification of mature follicles in female ovaries post egg-laying in controls expressing a WT *dVMAT* allele (grey) and the Δ3A *dVMAT*$^{\Delta 3}$ mutant (blue) derived from the same genetic background. Graphs show individual datapoints and group means, (WT n = 19 flies and Δ3A n = 20 flies, two-tailed unpaired *t*-test, $p \leq 0.0001$****). B. Location of the egg within the reproductive tract (RT) after 6 h of mating. Graphs show mean ± 95% confidence interval, (n = 54 flies for WT control and 60 flies for Δ3A), Fisher' exact test ($p \leq 0.001$***). C. Optogenetic stimulation of Tdc2-LexA » LexAop-ChR2-XXL in flies harboring *dVMAT*$^{\Delta 3}$ (Δ3A) mutant (blue) or a WT *dVMAT* allele derived from w^{1118} (black, Control/"Cont.") induces similar numbers of lateral oviduct contractions. (For interpretation of the references to colour in this figure legend, the reader is referred to the Web version of this article.)

possible that octopaminergic synapses in the CNS *upstream* of the reproductive tract are indirectly responsible for this phenotype. The methods we have established to express optogenetic and imaging transgenes in the *dVMAT*$^{\Delta 3}$ mutant background will be useful to explore upstream elements of the oviposition circuit in future experiments. Here, we have used optogenetics coupled with live imaging to analyze the effects of *dVMAT*$^{\Delta 3}$ on oviduct contractility *downstream* of ovulation. We do not detect a difference between *dVMAT*$^{\Delta 3}$ and wild type controls for the contraction of lateral oviduct muscle in response to optogenetic stimulation of octopaminergic neurons. These data indicate that at least one element of the oviposition circuit downstream of ovulation is not disrupted by *dVMAT*$^{\Delta 3}$. However, octopamine also regulates dilation of the oviducts, another process downstream of ovulation that may influence fertility (Rodriguez-Valentin et al., 2006; Deshpande et al., 2022). Dilation can be easily visualized when the reproductive tract is dissected out of the abdomen and octopamine is bath-applied to the reproductive tract (Rodriguez-Valentin et al., 2006; Deshpande et al., 2022). Unfortunately, visualization of dilation is difficult with the intact preparations that we have used here and are required for optogenetic stimulation of octopamine neurons within the abdominal ganglion (Deshpande et al., 2022). Since we cannot test the effects of *dVMAT*$^{\Delta 3}$ using bath-applied octopamine, we cannot rule out the possibility that *dVMAT*$^{\Delta 3}$ causes a defect in oviduct dilation.

In sum, while other aspects of the oviposition circuit may be disrupted by *dVMAT*$^{\Delta 3}$, our current data suggest that retention of mature eggs in the ovaries is likely to be responsible for the decrease in fertility. Moreover, at least some downstream processes such as oviduct contractions appear to be unaffected by a shift in octopamine release from SVs to LDCVs.

Since all of the aminergic neurotransmitters recognized by dVMAT–including dopamine, serotonin and octopamine– have been implicated in both feeding and survival, the mechanisms by which *dVMAT*$^{\Delta 3}$ causes alterations in these processes may be complex. Flies that lack octopamine have been shown to have substantially reduced lifespan (Li et al., 2016). Octopamine also regulates metabolic rate, physical activity, feeding rate, and food choice (Li et al., 2016) and both octopamine and serotonin regulate insulin secreting cells (Luo et al., 2012, 2014). Serotonin has been proposed to modulate food intake based on the pharmacological inhibition of the 5-HT2A receptor (Gasque et al., 2013) and mutation of 5-HT2A receptor decreases protein feeding and extends lifespan (Munneke et al., 2022). Activation of a small subset of serotonergic neurons can induce flies to feed regardless of satiation and may encode hunger (Albin et al., 2015). Dopaminergic neurons signaling in the mushroom body have been implicated in learning and memory of nutrients and sweet taste (Huetteroth et al., 2015; Yamagata et al., 2015). We speculate that some of these circuits may be disrupted in the *dVMAT*$^{\Delta 3}$ mutants, and that this may be responsible for reduced lifespan and increased feeding that we observe, but further experiments will be needed to explore specific pathways.

In future experiments, we will use additional drivers to express RCaMP in subsets of additional neurons to analyze the effects of *dVMAT*$^{\Delta 3}$ on aminergic circuits unrelated to oviposition, including those shown to regulate feeding and survival. Other circuits of interest include an octopaminergic pathway in the visual system that regulates the response of flies to odor plumes during flight (Wasserman et al., 2015). Ongoing experiments will determine whether *the dVMAT*$^{\Delta 3}$ line replicates the visual behavior phenotype that we have previously seen using a *UAS-DVMAT-Δ3* transgene (Wasserman et al., 2015). If so, expression of RCaMP in visual system neurons combined with *dVMAT*$^{\Delta 3}$ may be used to investigate the underlying mechanisms.

Our previous data indicates that the *dVMAT-Δ3* transgene traffics less to SVs, and we speculate that some aspects of the *dVMAT*$^{\Delta 3}$ phenotype is due to a decrease in amine release from SVs. However, in addition to a decrease in sorting to SVs, we have previously shown that the *dVMAT−Δ3* transgene localizes more to LDCVs than the wild type transporter (Grygoruk et al., 2014). Therefore, it is possible that increase

in amine release from LDCVs may also contribute to the *dVMAT*$^{\Delta 3}$ phenotype. Further experiments using mutations that more specifically disrupt sorting to SVs, may resolve this issue. Alternatively, it may not be possible to reduce dVMAT sorting to SVs without increasing its localization to LDCVs; another mutation (Y600A) also led to an increase in the localization of dVMAT to LDCVs (Grygoruk et al., 2014). We speculate that, at least in flies, there may be communication between the pathways for biogenesis and/or recycling of SVs and LDCVs, and at present, we can only conclude that the *dVMAT*$^{\Delta 3}$ phenotype results from a change in the balance of amine release between SVs and LDCVs.

The variety of octopamine-dependent processes within the oviposition circuit and the CNS provide a model to further probe the effects of dVMAT trafficking on circuit function. We speculate that further experiments using *dVMAT*$^{\Delta 3}$ coupled with optogenetics and imaging will help to elucidate the circuit properties that govern synaptic versus extrasynaptic signaling.

4. Methods

4.1. Husbandry

Mixed populations of male and female flies were raised on cornmeal-molasses agar media at 25 °C and 20–40% humidity with a 12-h light/dark cycle.

4.2. Mutagenesis and screening

Potential sites for CRISPS-Cas9 based mutagenesis in the *dVMAT* gene were selected using the online program CRISPR Optimal Target Finder (http://targetfinder.flycrispr.neuro.brown.edu/) and the guide RNA sequence gattgcagTCTTTGATCTA. The guide RNA vector was constructed by self-annealing the oligonucleotide containing the guide sequence plus 5′ and 3' recognition sites for the expression vector (CTTCgattgcagTCTTTGATCTA) and its reverse complement (TAGATCAAAGActgcaatc-CAAA), followed by ligation into a unique BbsI site in the vector pU6-2-BbsI-chiRNA (Gratz et al., 2013). The single guide RNA plasmid was co-injected (Best Gene, Inc.) with the 90-nt single-stranded repair oligonucleotide acccatacccttttccatttcatttctgtgattgcagTCTTAGATCTGCAGACGCGATCGGGCTCAGGTACGTTATGTAACCTATCAAAA (mutated bases underlined) into *vas-Cas9* expressing embryos (BDSC #51323). Of the 120 injected embryos,100 survived to adulthood and were mated to the balancer line *Tft/CyO* for two generations to obtain 450 stable lines expressing the mutagenized chromosome over *CyO*. To phenotypically screen for the presence of a *dVMAT* mutant, individual females from each line homozygous for the mutagenized chromosome were mated to wild type (Canton S) males and vials were visually inspected for evidence of reduced fertility and fecundity. To verify the presence of the mutation and the absence of spurious changes, genomic DNA from each one of the 57 lines was isolated and subjected to PCR using the primers TATGTATGCTCCATTGCTGACG and CCAAAGAAGGACTCTCACAAGC. PCR products were digested with BglII (NEB) followed by gel electrophoresis and/or DNA sequencing using the oligo TATGTATGCTCCATTGCTGACG (Genewiz).

4.3. Western blots

For western blots, 10 heads per genotype (5 males, 5 females) from flies aged 3–7 days were homogenized in 140 mM NaCl, 10 mM Tris-Cl pH 8.0, 0.5 mM EGTA, 1% Tx-100, 0.1% sodium deoxycholate, 0.1% SDS, with a protease inhibitor cocktail (Roche cOmplete Mini). Following centrifugation to remove debris (13000g, 5 min, ambient temperature) the supernatant was mixed with 1/5 volume of 5X SDS-PAGE sample buffer. One head-equivalent per lane was loaded on a 10% polyacrylamide gel and transferred to nitrocellulose. The top and bottom portions of the blot were probed with a rabbit primary antibody to the dVMAT amino terminus (1:1000 (Romero-Calderón et al., 2008),) or mouse anti-CSP (1:1000, Developmental Studies Hybridoma Bank) respectively (2 h, RT) followed by the appropriate HRP-conjugated secondary antibodies (anti-mouse, 1:2000, MEMD Millipore Corp, anti-rabbit, 1:2000, Invitrogen). The blot was washed and exposed to the HRP substrate SuperSignal West Pico PLUS (Thermo Scientific) and imaged on an Azure Biosystems C400 scanner. The area under the peak of bands representing dVMAT and CSP were quantified (ImageJ/Fiji) and dVMAT signal normalized to the CSP loading control for comparison across samples.

4.4. Larval locomotion

Two to three larvae were placed on the food for 30 s to acclimate and locomotion was scored as the number of 0.4 cm grids crossed over 2 min. Their speed was calculated as centimeters per second (cm/s) using Multi-Worm Tracker software (Swierczek et al., 2011).

4.5. Survival

Flies were housed in vials (5 males, 5 females per vial) and scored for survival each day until all flies were dead. Two hundred flies per genotype were tested.

4.6. Fertility

Flies were collected under CO_2 anesthesia 0–5 days before mating. One virgin female was mated with four w^{1118} males in vials at room temperature. Twelve days after mating, parents were removed. Candidates were scored as fertile if the vial contained at least one larva, pupa, or adult over the subsequent twelve days. A population of 70 flies were tested five times in replicate experiments. Fertility is expressed as the proportion of the population capable of producing at least one viable progeny.

4.7. Fecundity

Five females of the indicated genotype were mated to five w^{1118} control males in a vial for 3 days. Mated flies were passed into a new vial each day for 12 days. The number of eggs laid per vial on each day was scored manually. Twenty flies per genotype were tested and the number of eggs were counted each day for 12 days. Fecundity is expressed as number of eggs laid per female per day over 12 days.

4.8. Mature follicle quantification

Five-day-old females fed with wet yeast for one day and mated to 10 wild type Canton S males (5 females: 10 males) in bottles. After two days, ovaries were dissected from twenty flies per genotype, stained with DAPI, and mounted, with stage 14 mature follicles within each ovary quantified as described (Deady and Sun, 2015).

4.9. Egg distribution within the reproductive tract

To determine the location of the egg in the reproductive tract, single-pair matings were set up between one virgin female and one Canton S male. Flies were allowed to mate for 6 h, an interval sufficient for all females to reach a steady state level of ovulation and egg laying (Deady and Sun, 2015; Sun and Spradling, 2013). Females were then frozen (−80 °C, 5 min) and reproductive tracts were dissected to examine the location of the eggs.

4.10. Optogenetics and live-imaging

All flies used for optogenetic experiments contained two copies of *Tdc2-LexA* and one copy each of, *LexAop-ChR2-XXL, 24B-GAL4, and UAS-RCaMP1b* and were homozygous for either *dVMAT*$^{\Delta 3}$ or a wild type

dVMAT allele. In contrast to the behavioral experiments in which the WT *dVMAT* allele was contained within the same genetic background as $dVMAT^{\Delta 3}$, *the* WT *dVMAT* allele used in the optogenetic experiments was contained within the transgenic parents and thus originally derived from w^{1118}. Mixed cultures of males and female flies were reared in low-light conditions (to avoid uncontrolled stimulation of ChR2) on standard cornmeal-molasses agar media containing 80μM retinol for 2 days, from 4 to 6 days post-eclosion. At 6 days post-eclosion female flies were pinned, ventral side up to a Sylgard platform and immersed in HL3.1 as described (Deshpande et al., 2022). The ventral cuticle at the junction between the thorax and abdomen and a portion of the abdomen was carefully removed to expose the abdominal ganglion and the oviducts respectively. The preparations were imaged using an upright Zeiss AxioExaminer microscope fitted with a 10× immersion objective and a custom filter set that included a dual band excitation filter with peaks at 484 nm and 561 nm (FF01-484/561), a 593 nm high pass dichroic (FF593-Di03), and the single band emission filter (FF01-620/52). Two collimated LED light sources (565 nm and 470 nm, Thorlabs) were coupled using a "custom multi-LED source for microscope illumination" and passed through the epifluorescence light path of the microscope for visualization of the oviducts or optogenetic stimulation respectively. Following 1 min of baseline recording, optogenetic stimulation using the 470 nm LED was initiated manually via the driver (DC2200, Thorlabs) for 30 s followed by a 30 s rest period and a second 30 s stimulation period. Contractions were manually counted as described (Deshpande et al., 2022).

4.11. Feeding assay

Groups of ten flies 3-5-days old were starved for 24 h on 1% agar medium as a water source. After starvation, flies were transferred to blue food (10% sucrose, 5% active yeast, 1% agar, and 4% blue food dye (McCormick) and allowed to feed for 15 min. The amount of blue food dye ingested was measured using spectrophotometric measurement of the blue dye as previously described (Albin et al., 2003). In brief, 10 flies were homogenized in 400 μL PBS and centrifuged (14,000 rpm for 3 min at ambient temperature). 250 μL of the supernatant was aspirated into a fresh tube, avoiding the pelleted debris and re-centrifuged (14,000 rpm, 3 min, at ambient temperature). 200 μL of the supernatant was loaded into a 96 well microplate for absorbance readings (Biotek Synergy 2 Multi-Mode Plate Reader). The corrected absorbance of the dye was calculated by subtracting the absorbance at 750 nm (outside of blue dye profile) from the absorbance at 630 nm (peak of blue dye) as previously described (Albin et al., 2003).

Funding

This work was funded by R01MH107390 and R01MH114017 to DEK, T32GM008042, T32DA024635 and F30MH115609 to JDA, T32DA024635 to EWR and F32NS123014 to EMK.

CRediT authorship contribution statement

James D. Asuncion: Writing – original draft, led the mutagenesis, biochemical and behavioral experiments, performed the original screen. **Aditya Eamani:** performed the original screen, quantitated fertility and fecundity. **Ethan W. Rohrbach:** performed the optogenetic experiments. **Elizabeth M. Knapp:** performed additional behavioral experiments. **Sonali A. Deshpande:** performed additional behavioral experiments. **Shivan L. Bonanno:** assisted with biochemical assays and. **Jeremy E. Murphy:** assisted with behavioral assays. **Hakeem O. Lawal:** performed additional behavioral experiments. **David E. Krantz:** oversaw the project and edited the manuscript.

Declaration of competing interest

The authors declare that they have no known competing financial interests or personal relationships that could have appeared to influence the work reported in this paper.

Data availability

Data will be made available on request.

Acknowledgements

The authors would like to thank Maureen Sampson, Katherine Myers Gschweng, Daniel James Suto, Prarnathi Rao, and Melissa Trieu for their help and insight.

References

Albin, R.L., Koeppe, R.A., Bohnen, N.I., Nichols, T.E., Meyer, P., Wernette, K., Minoshima, S., Kilbourn, M.R., Frey, K.A., 2003. Increased ventral striatal monoaminergic innervation in Tourette syndrome. Neurology 61 (3), 310–315. http://www.ncbi.nlm.nih.gov/entrez/query.fcgi?cmd=Retrieve&db=PubMed&dopt=Citation&list_uids=12913189.

Albin, S.D., Kaun, K.R., Knapp, J.M., Chung, P., Heberlein, U., Simpson, J.H., 2015. A subset of serotonergic neurons evokes hunger in adult Drosophila. Curr. Biol. 25 (18), 2435–2440. https://www.ncbi.nlm.nih.gov/pubmed/26344091.

Avila, F.W., Bloch Qazi, M.C., Rubinstein, C.D., Wolfner, M.F., 2012. A requirement for the neuromodulators octopamine and tyramine in Drosophila melanogaster female sperm storage. Proc. Natl. Acad. Sci. U. S. A. 109 (12), 4562–4567. http://www.ncbi.nlm.nih.gov/entrez/query.fcgi?cmd=Retrieve&db=PubMed&dopt=Citation&list_uids=22393023.

Blakely, R.D., Edwards, R.H., 2012. Vesicular and plasma membrane transporters for neurotransmitters. Cold Spring Harbor Perspect. Biol. 4 (2), 22199021. http://www.ncbi.nlm.nih.gov/entrez/query.fcgi?cmd=Retrieve&db=PubMed&dopt=Citation&list_uids=22199021.

Boel, A., De Saffel, H., Steyaert, W., Callewaert, B., De Paepe, A., Coucke, P.J., Willaert, A., 2018. CRISPR/Cas9-mediated homology-directed repair by ssODNs in zebrafish induces complex mutational patterns resulting from genomic integration of repair-template fragments. Dis. Mod. Mech. 11 (10). PMC6215429.

Bowton, E., Saunders, C., Reddy, I.A., Campbell, N.G., Hamilton, P.J., Henry, L.K., Coon, H., Sakrikar, D., Veenstra-VanderWeele, J.M., Blakely, R.D., Sutcliffe, J., Matthies, H.J., Erreger, K., Galli, A., 2014. SLC6A3 coding variant Ala559Val found in two autism probands alters dopamine transporter function and trafficking. Transl. Psychiatry 4 (10), e464. PMC4350523.

Bu, M., Farrer, M.J., Khoshbouei, H., 2021. Dynamic control of the dopamine transporter in neurotransmission and homeostasis. NPJ Parkinsons Dis. 7 (1), 22. PMC7935902.

Chang, H.-Y., Grygoruk, A., Brooks, E.S., Ackerson, L.C., Maidment, N.T., Bainton, R.J., Krantz, D.E., 2006. Over-expression of the Drosophila vesicular monoamine transporter increases motor activity and courtship but decreases the behavioral response to cocaine. Mol. Psychiatr. 11, 99–113.

Cole, S.H., Carney, G.E., McClung, C.A., Willard, S.S., Taylor, B.J., Hirsh, J., 2005. Two functional but noncomplementing Drosophila tyrosine decarboxylase genes: distinct roles for neural tyramine and octopamine in female fertility. J. Biol. Chem. 280 (15), 14948–14955. http://www.ncbi.nlm.nih.gov/entrez/query.fcgi?cmd=Retrieve&db=PubMed&dopt=Citation&list_uids=15691831.

Cong, L., Ran, F.A., Cox, D., Lin, S., Barretto, R., Habib, N., Hsu, P.D., Wu, X., Jiang, W., Marraffini, L.A., Zhang, F., 2013. Multiplex genome engineering using CRISPR/Cas systems. Science 339 (6121), 819–823. PMC3795411.

Deady, L.D., Sun, J., 2015. A follicle rupture assay reveals an essential role for follicular adrenergic signaling in Drosophila ovulation. PLoS Genet. 11 (10), e1005604. PMC4608792.

Deshpande, S.A., Rohrbach, E.W., Asuncion, J.D., Harrigan, J., Eamani, A., Schlingmann, E.H., Suto, D.J., Lee, P.T., Schweizer, F.E., Bellen, H.J., Krantz, D.E., 2022. Regulation of Drosophila oviduct muscle contractility by octopamine. iScience 25 (8), 104697. PMC9307614.

Dittman, J.S., Ryan, T.A., 2019. The control of release probability at nerve terminals. Nat. Rev. Neurosci. 20 (3), 177–186. https://www.ncbi.nlm.nih.gov/pubmed/30647451.

Duerr, J.S., Frisby, D.L., Gaskin, J., Duke, A., Asermely, K., Huddleston, D., Eiden, L.E., Rand, J.B., 1999. The cat-1 gene of Caenorhabditis elegans encodes a vesicular monoamine transporter required for specific monoamine-dependent behaviors. J. Neurosci. 19, 72–84.

Fagan, R.R., Kearney, P.J., Melikian, H.E., 2020. In situ regulated dopamine transporter trafficking: there's No place like home. Neurochem. Res. 45 (6), 1335–1343. PMC7261626.

Fischer, F.P., Kasture, A.S., Hummel, T., Sucic, S., 2022. Molecular and clinical repercussions of GABA transporter 1 variants gone amiss: links to epilepsy and developmental spectrum disorders. Front. Mol. Biosci. 9, 834498. PMC7612498.

Fuxe, K., Dahlstrom, A.B., Jonsson, G., Marcellino, D., Guescini, M., Dam, M., Manger, P., Agnati, L., 2010. The discovery of central monoamine neurons gave volume transmission to the wired brain. Prog. Neurobiol. 90 (2), 82–100. http://www.ncbi.

nlm.nih.gov/entrez/query.fcgi?cmd=Retrieve&db=PubMed&dopt=Citation&list_uids=19853007.
Gasque, G., Conway, S., Huang, J., Rao, Y., Vosshall, L.B., 2013. Small molecule drug screening in Drosophila identifies the 5HT2A receptor as a feeding modulation target. Sci. Rep. 3 srep.02120. http://www.ncbi.nlm.nih.gov/entrez/query.fcgi?cmd=Retrieve&db=PubMed&dopt=Citation&list_uids=23817146.
Gotze, K.J., Mrestani, A., Beckmann, P., Krohn, K., Le Duc, D., Velluva, A., Bohme, M.A., Heckmann, M., Abou Jamra, R., Lemke, J.R., Blaker, H., Scholz, N., Ljaschenko, D., Langenhan, T., 2022. Improving one-step scarless genome editing in Drosophila melanogaster by combining ovo(D) co-CRISPR selection with sgRNA target site masking. Biol. Method. Protoc. 7 (1) bpac003. PMC8789338.
Gowrishankar, R., Gresch, P.J., Davis, G.L., Katamish, R.M., Riele, J.R., Stewart, A.M., Vaughan, R.A., Hahn, M.K., Blakely, R.D., 2018. Region-specific regulation of presynaptic dopamine homeostasis by D(2) autoreceptors shapes the in vivo impact of the neuropsychiatric disease-associated DAT variant Val559. J. Neurosci. 38 (23), 5302–5312. PMC5990980.
Gratz, S.J., Cummings, A.M., Nguyen, J.N., Hamm, D.C., Donohue, L.K., Harrison, M.M., Wildonger, J., O'Connor-Giles, K.M., 2013. Genome engineering of Drosophila with the CRISPR RNA-guided Cas9 nuclease. Genetics 194 (4), 1029–1035. http://www.ncbi.nlm.nih.gov/entrez/query.fcgi?cmd=Retrieve&db=PubMed&dopt=Citation&list_uids=23709638.
Greer, C.L., Grygoruk, A., Patton, D.E., Ley, B., Romero-Calderón, R., Chang, H.-Y., Houshyar, R., Bainton, R.J., DiAntonio, A., Krantz, D.E., 2005. A splice variant of the Drosophila vesicular monoamine transporter contains a conserved trafficking domain and functions in the storage of dopamine, serotonin and octopamine. J. Neurobiol. 64, 239–258.
Grygoruk, A., Fei, H., Daniels, R.W., Miller, B.R., Diantonio, A., Krantz, D.E., 2010. A tyrosine-based motif localizes a Drosophila vesicular transporter to synaptic vesicles in vivo. J. Biol. Chem. 285 (10), 6867–6878. http://www.ncbi.nlm.nih.gov/entrez/query.fcgi?cmd=Retrieve&db=PubMed&dopt=Citation&list_uids=20053989.
Grygoruk, A., Chen, A., Martin, C.A., Lawal, H.O., Fei, H., Gutierrez, G., Biedermann, T., Najibi, R., Hadi, R., Chouhan, A.K., Murphy, N.P., Schweizer, F.E., Macleod, G.T., Maidment, N.T., Krantz, D.E., 2014. The redistribution of Drosophila vesicular monoamine transporter mutants from synaptic vesicles to large dense-core vesicles impairs amine-dependent behaviors. J. Neurosci. 34 (20), 6924–6937. http://www.ncbi.nlm.nih.gov/entrez/query.fcgi?cmd=Retrieve&db=PubMed&dopt=Citation&list_uids=24828646.
Haase, J., Jones, A.K.C., Mc Veigh, C.J., Brown, E., Clarke, G., Ahnert-Hilger, G., 2021. Sex and brain region-specific regulation of serotonin transporter activity in synaptosomes in guanine nucleotide-binding protein G(q) alpha knockout mice. J. Neurochem. 159 (1), 156–171. https://www.ncbi.nlm.nih.gov/pubmed/34309872.
Hana, S., Lange, A.B., 2017. Octopamine and tyramine regulate the activity of reproductive visceral muscles in the adult female blood-feeding bug, Rhodnius prolixus. J. Exp. Biol. 220 (10), 1830–1836. https://www.ncbi.nlm.nih.gov/pubmed/28235907.
Huetteroth, W., Perisse, E., Lin, S., Klappenbach, M., Burke, C., Waddell, S., 2015. Sweet taste and nutrient value subdivide rewarding dopaminergic neurons in Drosophila. Curr. Biol. 25 (6), 751–758. PMC4372253.
Ingram, S.M., Rana, T., Manson, A.M., Yayah, F.M., Jackson, E.G.B., Anderson, C., Davids, B.O., Goodwin, J.S., 2021. Optogenetically-induced multimerization of the dopamine transporter increases uptake and trafficking to the plasma membrane. J. Biol. Chem. 296, 100787. PMC8203837.
Janickova, H., Prado, V.F., Prado, M.A.M., El Mestikawy, S., Bernard, V., 2017. Vesicular acetylcholine transporter (VAChT) over-expression induces major modifications of striatal cholinergic interneuron morphology and function. J. Neurochem. 142 (6), 857–875. https://www.ncbi.nlm.nih.gov/pubmed/28628197.
Kasture, A.S., Bartel, D., Steinkellner, T., Sucic, S., Hummel, T., Freissmuth, M., 2019. Distinct contribution of axonal and somatodendritic serotonin transporters in drosophila olfaction. Neuropharmacology 161, 107564. https://www.ncbi.nlm.nih.gov/pubmed/30851308.
Lee, H.G., Seong, C.S., Kim, Y.C., Davis, R.L., Han, K.A., 2003. Octopamine receptor OAMB is required for ovulation in Drosophila melanogaster. Dev. Biol. 264 (1), 179–190. http://www.ncbi.nlm.nih.gov/entrez/query.fcgi?cmd=Retrieve&db=PubMed&dopt=Citation&list_uids=14623240.
Lee, H.G., Rohila, S., Han, K.A., 2009. The octopamine receptor OAMB mediates ovulation via Ca2+/calmodulin-dependent protein kinase II in the Drosophila oviduct epithelium. PLoS One 4 (3), e4716. http://www.ncbi.nlm.nih.gov/entrez/query.fcgi?cmd=Retrieve&db=PubMed&dopt=Citation&list_uids=19262750.
Levi, T., Sloutskin, A., Kalifa, R., Juven-Gershon, T., Gerlitz, O., 2020. Efficient in vivo introduction of point mutations using ssODN and a Co-CRISPR approach. Biol. Proced. Online 22, 14. PMC7362497.
Li, Y., Hoffmann, J., Li, Y., Stephano, F., Bruchhaus, I., Fink, C., Roeder, T., 2016. Octopamine controls starvation resistance, life span and metabolic traits in Drosophila. Sci. Rep. 6, 35359. PMC5069482.
Li, H., Datunashvili, M., Reyes, R.C., Voglmaier, S.M., 2022. Inositol hexakisphosphate kinases differentially regulate trafficking of vesicular glutamate transporters 1 and 2. Front. Cell. Neurosci. 16, 926794. PMC9355605.
Lim, J., Sabandal, P.R., Fernandez, A., Sabandal, J.M., Lee, H.G., Evans, P., Han, K.A., 2014. The octopamine receptor Octbeta2R regulates ovulation in Drosophila melanogaster. PLoS One 9 (8), e104441. http://www.ncbi.nlm.nih.gov/entrez/query.fcgi?cmd=Retrieve&db=PubMed&dopt=Citation&list_uids=25099506.
Liu, Y., Edwards, R.H., 1997. The role of vesicular transport proteins in synaptic transmission and neural degeneration. Annu. Rev. Neurosci. 20, 125–156.
Luo, J., Becnel, J., Nichols, C.D., Nassel, D.R., 2012. Insulin-producing cells in the brain of adult Drosophila are regulated by the serotonin 5-HT1A receptor. Cell. Mol. Life Sci. 69 (3), 471–484. PMC3934008.
Luo, J., Lushchak, O.V., Goergen, P., Williams, M.J., Nassel, D.R., 2014. Drosophila insulin-producing cells are differentially modulated by serotonin and octopamine receptors and affect social behavior. PLoS One 9 (6), e99732. PMC4055686.
Meinke, C., Quinlan, M.A., Paffenroth, K.C., Harrison, F.E., Fenollar-Ferrer, C., Katamish, R.M., Stillman, I., Ramamoorthy, S., Blakely, R.D., 2022. Serotonin transporter Ala276 mouse: novel model to assess the neurochemical and behavioral impact of Thr276 phosphorylation in vivo. Neurochem. Res. 47 (1), 37–60. https://www.ncbi.nlm.nih.gov/pubmed/33830406.
Middleton, A., Nongthomba, U., Parry, K., Sweeney, S.T., Sparrow, J.C., Elliott, C.J., 2006. Neuromuscular organization and aminergic modulation of contractions in the Drosophila ovary. BMC Biol. 4 (1), 17. http://www.ncbi.nlm.nih.gov/entrez/query.fcgi?cmd=Retrieve&db=PubMed&dopt=Citation&list_uids=16768790.
Moron, J.A., Zakharova, I., Ferrer, J.V., Merrill, G.A., Hope, B., Lafer, E.M., Lin, Z.C., Wang, J.B., Javitch, J.A., Galli, A., Shippenberg, T.S., 2003. Mitogen-activated protein kinase regulates dopamine transporter surface expression and dopamine transport capacity. J. Neurosci. 23 (24), 8480–8488. PMC6740378.
Munneke, A.S., Chakraborty, T.S., Porter, S.S., Gendron, C.M., Pletcher, S.D., 2022. The serotonin receptor 5-HT2A modulates lifespan and protein feeding in Drosophila melanogaster. Front. Aging 3, 1068455. PMC9751412.
Paquet, D., Kwart, D., Chen, A., Sproul, A., Jacob, S., Teo, S., Olsen, K.M., Gregg, A., Noggle, S., Tessier-Lavigne, M., 2016. Efficient introduction of specific homozygous and heterozygous mutations using CRISPR/Cas9. Nature 533 (7601), 125–129. https://www.ncbi.nlm.nih.gov/pubmed/27120160.
Pauls, D., Blechschmidt, C., Frantzmann, F., El Jundi, B., Selcho, M., 2018. A comprehensive anatomical map of the peripheral octopaminergic/tyraminergic system of Drosophila melanogaster. Sci. Rep. 8 (1), 15314. PMC6192984.
Ragu Varman, D., Jayanthi, L.D., Ramamoorthy, S., 2021. Glycogen synthase kinase-3ss supports serotonin transporter function and trafficking in a phosphorylation-dependent manner. J. Neurochem. 156 (4), 445–464. PMC7882002.
Rezaval, C., Nojima, T., Neville, M.C., Lin, A.C., Goodwin, S.F., 2014. Sexually dimorphic octopaminergic neurons modulate female postmating behaviors in Drosophila. Curr. Biol. 24 (7), 725–730. http://www.ncbi.nlm.nih.gov/pubmed/24631243.
Rodriguez-Valentin, R., Lopez-Gonzalez, I., Jorquera, R., Labarca, P., Zurita, M., Reynaud, E., 2006. Oviduct contraction in Drosophila is modulated by a neural network that is both, octopaminergic and glutamatergic. J. Cell. Physiol. 209 (1), 183–198. http://www.ncbi.nlm.nih.gov/entrez/query.fcgi?cmd=Retrieve&db=PubMed&dopt=Citation&list_uids=16826564.
Romero-Calderón, R., Uhlenbrock, G., Boryz, J., Simon, A.F., Grygoruk, A., Yee, S.K., Shyer, A., Ackerson, L.C., Maidment, N.T., Meinertzhagen, I.A., Hovemann, B.T., Krantz, D.E., 2008. A glial variant of the vesicular monoamine transporter is required to store histamine in the Drosophila visual system. PLoS Genet. 4 (11), e1000245. PMC2570955.
Sebo, Z.L., Lee, H.B., Peng, Y., Guo, Y., 2013. A simplified and efficient germline-specific CRISPR/Cas9 system for Drosophila genomic engineering. Fly (Austin) 8 (1). http://www.ncbi.nlm.nih.gov/entrez/query.fcgi?cmd=Retrieve&db=PubMed&dopt=Citation&list_uids=24141137.
Simon, A.F., Daniels, R., Romero-Calderón, R., Grygoruk, A., Chang, H.Y., Najibi, R., Shamouelian, D., Salazar, E.D., Solomon, M., Ackerson, L.C., Maidment, N.T., Diantonio, A., Krantz, D.E., 2008. Drosophila Vesicular Monoamine Transporter Mutants Can Adapt to Reduced or Eliminated Vesicular Stores of Dopamine and Serotonin. Genetics. http://www.ncbi.nlm.nih.gov/entrez/query.fcgi?cmd=Retrieve&db=PubMed&dopt=Citation&list_uids=19033154.
Simon, A.F., Daniels, R., Romero-Calderón, R., Grygoruk, A., Chang, H.Y., Najibi, R., Shamouelian, D., Salazar, E., Solomon, M., Ackerson, L.C., Maidment, N.T., Diantonio, A., Krantz, D.E., 2009. Drosophila vesicular monoamine transporter mutants can adapt to reduced or eliminated vesicular stores of dopamine and serotonin. Genetics 181 (2), 525–541. http://www.ncbi.nlm.nih.gov/entrez/query.fcgi?cmd=Retrieve&db=PubMed&dopt=Citation&list_uids=19033154.
Soldner, F., Laganiere, J., Cheng, A.W., Hockemeyer, D., Gao, Q., Alagappan, R., Khurana, V., Golbe, L.I., Myers, R.H., Lindquist, S., Zhang, L., Guschin, D., Fong, L.K., Vu, B.J., Meng, X., Urnov, F.D., Rebar, E.J., Gregory, P.D., Zhang, H.S., Jaenisch, R., 2011. Generation of isogenic pluripotent stem cells differing exclusively at two early onset Parkinson point mutations. Cell 146 (2), 318–331. PMC3155290.
Sun, J., Spradling, A.C., 2013. Ovulation in Drosophila is controlled by secretory cells of the female reproductive tract. Elife 2, e00415. PMC3628084.
Sun, M., Han, X., Chang, F., Xu, H., Colgan, L., Liu, Y., 2020. Regulatory role of sorting nexin 5 in protein stability and vesicular targeting of vesicular acetylcholine transporter to synaptic vesicle-like vesicles in PC12 cells. J. Biomed. Res. 35 (5), 339–350. PMC8502691.
Swierczek, N.A., Giles, A.C., Rankin, C.H., Kerr, R.A., 2011. High-throughput behavioral analysis in C. elegans. Nat. Methods 8 (7), 592–598. http://www.ncbi.nlm.nih.gov/entrez/query.fcgi?cmd=Retrieve&db=PubMed&dopt=Citation&list_uids=21642964.
Touroutine, D., Tanis, J.E., 2020. A rapid, SuperSelective method for detection of single nucleotide variants in Caenorhabditis elegans. Genetics 216 (2), 343–352. PMC7536863.
Trueta, C., Kuffler, D.P., De-Miguel, F.F., 2012. Cycling of dense core vesicles involved in somatic exocytosis of serotonin by leech neurons. Front. Physiol. 3, 175. http://www.ncbi.nlm.nih.gov/entrez/query.fcgi?cmd=Retrieve&db=PubMed&dopt=Citation&list_uids=22685436.
Wasserman, S.M., Aptekar, J.W., Lu, P., Nguyen, J., Wang, A.L., Keles, M.F., Grygoruk, A., Krantz, D.E., Larsen, C., Frye, M.A., 2015. Olfactory neuromodulation of motion vision circuitry in Drosophila. Curr. Biol. 25 (4), 467–472. PMC4331282.

White, M.A., Chen, D.S., Wolfner, M.F., 2021. She's got nerve: roles of octopamine in insect female reproduction. J. Neurogenet. 35 (3), 132–153. PMC8455407.
Wu, S., Bellve, K.D., Fogarty, K.E., Melikian, H.E., 2015. Ack1 is a dopamine transporter endocytic brake that rescues a trafficking-dysregulated ADHD coding variant. Proc. Natl. Acad. Sci. U. S. A. 112 (50), 15480–15485. PMC4687542.
Xie, F., Ye, L., Chang, J.C., Beyer, A.I., Wang, J., Muench, M.O., Kan, Y.W., 2014. Seamless gene correction of beta-thalassemia mutations in patient-specific iPSCs using CRISPR/Cas9 and piggyBac. Genome Res. 24 (9), 1526–1533. PMC4158758.
Xu, H., Chang, F., Jain, S., Heller, B.A., Han, X., Liu, Y., Edwards, R.H., 2022. SNX5 targets a monoamine transporter to the TGN for assembly into dense core vesicles by AP-3. J. Cell Biol. 221 (5). PMC9016777.
Yamagata, N., Ichinose, T., Aso, Y., Placais, P.Y., Friedrich, A.B., Sima, R.J., Preat, T., Rubin, G.M., Tanimoto, H., 2015. Distinct dopamine neurons mediate reward signals for short- and long-term memories. Proc. Natl. Acad. Sci. U. S. A. 112 (2), 578–583. PMC4299218.
Yang, L., Guell, M., Byrne, S., Yang, J.L., De Los Angeles, A., Mali, P., Aach, J., Kim-Kiselak, C., Briggs, A.W., Rios, X., Huang, P.Y., Daley, G., Church, G., 2013. Optimization of scarless human stem cell genome editing. Nucleic Acids Res. 41 (19), 9049–9061. PMC3799423.
Ye, L., Wang, J., Beyer, A.I., Teque, F., Cradick, T.J., Qi, Z., Chang, J.C., Bao, G., Muench, M.O., Yu, J., Levy, J.A., Kan, Y.W., 2014. Seamless modification of wild-type induced pluripotent stem cells to the natural CCR5Delta32 mutation confers resistance to HIV infection. Proc. Natl. Acad. Sci. U. S. A. 111 (26), 9591–9596. PMC4084478.
Yoshinari, Y., Ameku, T., Kondo, S., Tanimoto, H., Kuraishi, T., Shimada-Niwa, Y., Niwa, R., 2020. Neuronal octopamine signaling regulates mating-induced germline stem cell increase in female Drosophila melanogaster. Elife 9. PMC7591258.
Yu, Z., Ren, M., Wang, Z., Zhang, B., Rong, Y.S., Jiao, R., Gao, G., 2013. Highly efficient genome modifications mediated by CRISPR/Cas9 in Drosophila. Genetics 195 (1), 289–291. http://www.ncbi.nlm.nih.gov/entrez/query.fcgi?cmd=Retrieve&db=PubMed&dopt=Citation&list_uids=23833182.